830-nm AlGaAs-InGaAs Graded Index Double Barrier Separate Confinement Heterostructures Laser Diodes With Improved Temperature and Divergence Characteristics

Chih-Tsang Hung, and Tien-Chang Lu, *Senior Member, IEEE*

***Abstract*— The 830-nm AlGaAs/InGaAs laser diodes (LDs) adopting multistep-graded index double-barrier separate confinement heterostructures (GRIN-DBSCHs) with small divergence beams and improved temperature characteristics under a high-output-power operation are reported. The double-barrier separate confinement heterostructure (DBSCH) design provides good carrier confinement and prevents current leakage by adding a multistep grading layer between cladding and waveguide layers. Simultaneously, the DBSCH design can facilitate reducing the divergence angle at high-power operation and widening the transverse mode distribution to decrease the power density around emission facets. In addition, the p-side doping depth is optimized to effectively raise the barrier height for reducing the electron overflow. Gaussian-like narrow far-field patterns are measured with the full-width at half-maximum vertical divergence angle to be between 11° and 13°. A threshold current of 16.5 mA and a slop efficiency of 0.98 W/A are obtained in the continuous-wave operation condition at room temperature. The maxima optical power densities of 21.5 MW/cm^2 per laser facet and good characteristic temperature values of threshold current (T_0) and slope efficiency (T_1) are achieved.**

***Index Terms*— AlGaAs-InGaAs heterostructure, laser beam divergence, laser diodes, quantum wells.**

I. Introduction

HIGH power AlGaAs-based laser diodes (LDs) are widely used as optical pump sources in various applications, such as solid state and fiber lasers. These applications require primarily high light output power and small beam divergence to achieve high conversion and coupling efficiency. In the direction perpendicular to the junction of LDs, the output beam characteristics are determined by the epitaxial growth and design which will affect the characteristics of high power operation of the laser diodes evidently. Normally, the narrow emission slot of optical power density in the near-field (NF) of LDs would contribute to a low catastrophic optical damage (COD) threshold level of the laser facet, and the corresponding far-field (FF) beam divergence is large. As a result, most of the high power LD applications would require the improved beam quality and reduced beam divergence to enable more efficient power collection or coupling efficiency. In addition, the COD level should be increased by preventing the negative effect resulted from the NF beam size reduction.

Various designs of laser heterostructures aiming at the beam divergence reduction and increase of the laser facet COD level have been proposed, such as utilization of a large optical cavity (LOC) into the separate-confinement heterostructure (SCH) epitaxial layers to broaden the optical mode distribution [1]–[4], inserting additional layers to control waveguide properties of conventional SCHs [5]–[8], and using the vertically integrated passive array [9]. For high power infrared LDs based on AlGaAs/InGaAs SCH designs, the LOC heterostructure have demonstrated multi-watt lasing capability successfully with a low vertical divergence beam. A marked drawback of LOC LDs is, however, the deterioration of the laser diode performance especially in decreasing of the slope efficiency and T_0 value as waveguide layers are designed excessively thick to reach very high power operation. Compared with the LOC design into SCH, the LDs with the double barrier separate confinement heterostructures (DBSCH) possess superior characteristics in both COD levels and beam divergence with only moderate deterioration of LD performance in slope efficiency and characteristic temperature [10].

The high power AlGaAs/InGaAs single quantum well (SQW) LDs adopting the DBSCH structures have demonstrated low vertical divergence angle; however, it caused a higher threshold and moderate increase in the resistance value due to deterioration of carrier confinement [10]. For the DBSCH design, a pair of wide-gap barrier layers possessing low refractive index is inserted into two interfaces between the waveguide and cladding layers. The double barriers can be utilized to weaken the optical confinement and shape the optical filed distribution in the vertical direction by modifying the epitaxial profile of double barriers. Since broadening of the mode distribution does not only reduce the far-field divergence angle but also raises the threshold current density, it is important to optimize the structure profile of double barriers to achieve small beam divergence and low threshold current simultaneously.

In this study, we adopted the DBSCH design and had optimized the thickness and barrier height to keep reducing

Manuscript received August 22, 2012; revised November 21, 2012; accepted November 25, 2012. Date of publication December 11, 2012; date of current version December 20, 2012. This work was supported in part by the Ministry of Education Aim for the Top University Program and the National Science Council of Taiwan under Contract NSC 99-2221-E-009-035-MY3.

The authors are with the Department of Photonics, Institute of Electro-Optical Engineering, National Chiao Tung University, Hsinchu 30050, Taiwan (e-mail: dolphone01@gmail.com; timtclu@mail.nctu.edu.tw).

Color versions of one or more of the figures in this paper are available online at http://ieeexplore.ieee.org.

Digital Object Identifier 10.1109/JQE.2012.2231053

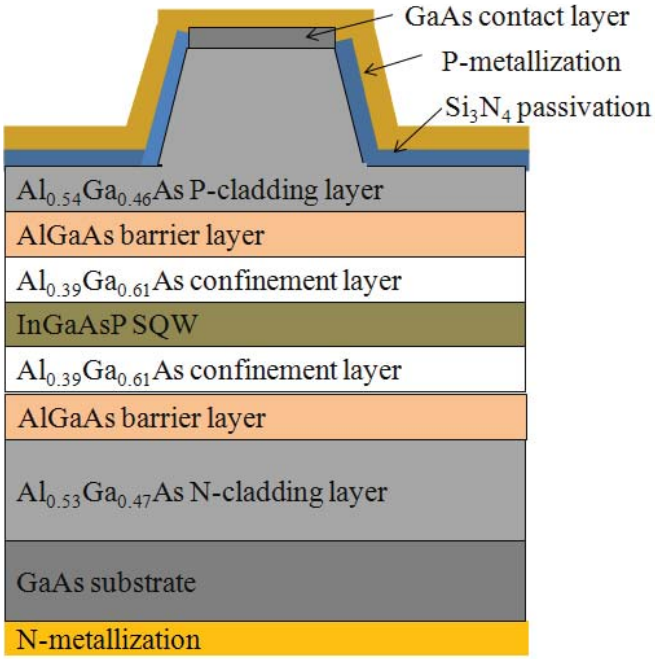

Fig. 1. Schematic of an 830-nm AlGaAs/InGaAs DBSCH ridge waveguide LD.

the vertical divergence angle less than 15°. We developed various DBSCH structures which the optical confinement factor was kept the same by adjusting the thickness of confining layers to achieve the similar FF divergence. For the optimized GRIN-DBSCH LD, threshold current of 16.5 mA and slope efficiency of 0.98 W/A have been obtained in the continuous-wave operation condition at room temperature and the maximal optical power density of 21.5 MW/cm^2 and good temperature sensitivity in terms of threshold current and slope efficiency variation have been achieved.

II. Experiment

Fig. 1 shows a schematic of a narrow stripe DBSCH LD for 830-nm band based on AlGaAs/InGaAs heterostructures. The active region containing a single tensile-strained $In_{0.01}Ga_{0.99}As_{0.995}P_{0.005}$ quantum well (QW) with a targeted thickness of 50 nm and composition to achieve the lasing wavelength of 830 nm was embedded in the confinement or waveguide layers made from AlGaAs. Comparing to conventional QW design, we adopt a thick active layer which quasi-Fermi level is relatively low and it contributes to less carrier leakage. Therefore, it also reduces the degradation of slope efficiency under high-temperature operation. Insertion of thin high Al content or wide-gap barrier layers can effectively modify the refractive index values at the interfaces between waveguide and cladding layers to control the optical confinement and the carrier confinement. The asymmetric cladding layers were adopted in this study, which composed of p-type $Al_{0.54}Ga_{0.46}As$ and n-type $Al_{0.53}Ga_{0.47}As$ layers, to on purpose lower the percentage of optical field in the p-type cladding layers which can reduce the free carrier absorption in the p-doped region. Above the p-cladding layer, high level carbon doped GaAs cap layer was used for the subsequent

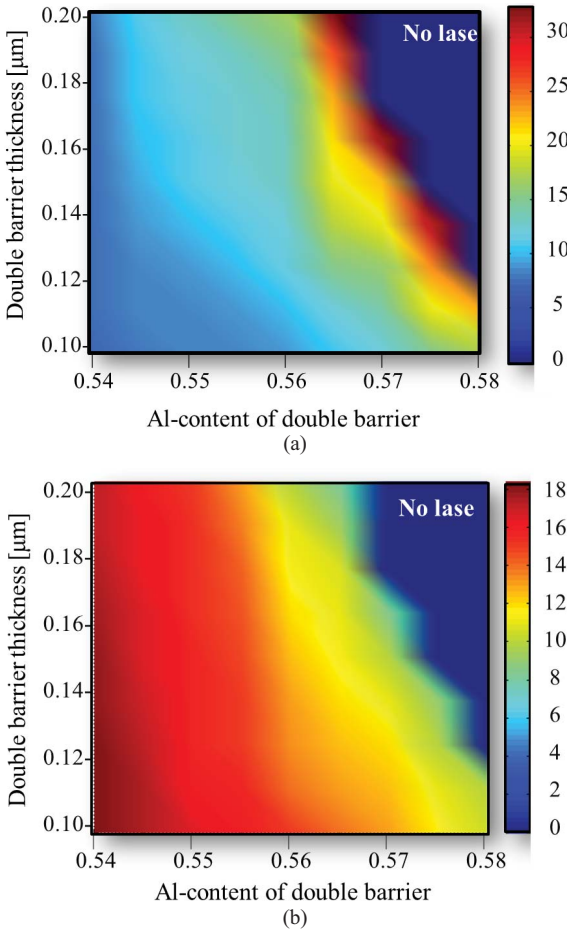

Fig. 2. 2-D mappings of (a) far-field vertical angles, and (b) threshold current in 830-nm AlGaAs/InGaAs DBSCH LDs as functions of the Al-content and thickness of double barriers in the X and Y axis. Deep blue regions: no lasing or extremely high-threshold conditions.

ohmic contact. The stripe width was set to be 5 μm and the cavity length was chosen as 500 μm. In this study, the NF optical mode profiles and LD characteristics were theoretically studied in detail by using an advanced LASer Technology Integrated Program (LASTIP), which self-consistently combined quantum well band structure calculations by 6 × 6 k.p theory, radiative and nonradiative carrier recombination, carrier drift and diffusion, and optical mode computation [11].

By inserting thin wide-gap (low refractive index) barrier layers into the SCH, the vertical optical mode profile will be broadened, which leads to a low optical confinement factor and increases the probability of the free carrier absorption loss in the cladding layers, thus contributing to the rising of threshold current. In order to obtain a suitable LD performance, we adjusted the profile of double-barriers to observe the effect on the far-field divergences angle and threshold current of LDs. Figs. 2(a) and (b) illustrate the two-dimensional (2D) mappings of the far-field vertical angle and threshold current as functions of the double barrier height (or Al composition) and thickness. It should be noted that the deep blue regions represent no lasing or the extremely high threshold conditions.

As modifying the barrier thickness from 0.1 to 0.2 μm and Al content from 0.54 to 0.58, the far-field angles of DBSCH LDs decreased gradually from 18° to 11°. Both of

the effects of increasing the barrier thickness or raising the barrier height can extend the near-field optical mode profile and contribute to the deterioration of the optical confinement factors. The near-field optical field distribution was expended and in consequence the emitted vertical beam divergence reduced gradually. The threshold current therefore rose from 10 mA to 33 mA with increasing either the barrier height or thickness. While the Al composition or thickness of the double barrier surpassed the threshold limit value, it became difficult to drive LDs in the lasing status and formed "no lase" regions located around the upper right sides of the 2D mappings in Fig. 2. According to the modeling results, it was proper to choose the composition and thickness of barrier layer to be $Al_{0.56}Ga_{0.44}As$ and 0.1-0.16 μm to satisfy the requirement that the output beam divergence angle was less than 15° as well as the threshold current was around 14 mA. The calculated fundamental mode distribution of DBSCH SQW design and the corresponding refractive index profile are shown in Fig. 3.

Based on the design of DBSCH structure shown in Fig. 1, we then modified the structures of double-barrier and waveguide layers to be graded refractive index (GRIN) DBSCH structures and multi-step GRIN-DBSCH structures to investigate the effect of carrier overflow and further improve the LD characteristics. The step-type composition profile was replaced by adding layers containing graded Al-content of AlGaAs into the interfaces between cladding, double barrier, and confinement layers. In addition, we adopted an asymmetrical design in p- and n-type cladding layers, where we slightly increased the Al-content of the p-cladding layer, bringing the optical mode profile to expand more into the n-cladding. As shown in Fig. 3, the optical field distribution is shifting away from the p-cladding layer, which should reduce the free carrier absorption loss caused by the heavy Zn doping concentration in the p-cladding layer. It could be beneficial to reduce the threshold current especially with increasing the barrier height and thickness. As indicated in Table I, we designed three confining layer structures. Version A, B and C had a step DBSCH, a linear GRIN-DBSCH, and a multi-step GRIN-DBSCH design, respectively. We on purposely modified the thickness of these three structures to keep the same optical confinement factor and to achieve the FF divergence angle less than 15°.

Fig. 4 shows the simulated carrier concentration of these DBSCH LDs above the threshold at the operation temperature of 300 K. It's interesting to note that the higher level electron concentration exists in the inner confinement layers for the multi-step DBSCH design, suggesting that most carriers have been limited to the regions close to the QW to obtain better electron injection. At the same time, a lower value of leakage electron concentration appears in the p-type cladding layer for the multi-step GRIN-DBSCH design, which results in a lower corresponding leakage current (not shown here) of 327.7 A/cm^2 in comparison to those of 433.1, 552.7 A/cm^2 for step DBSCH and linear GRIN-DBSCH LDs, respectively. As a result, the multi-step grading structure could bring the most effective restriction against the electron overflow.

According to the above modeling results, we fabricated different types DBSCH LDs in a low pressure metal-organic

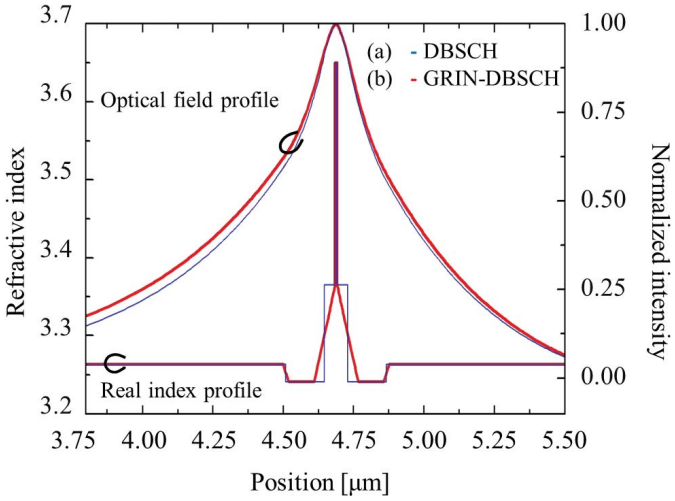

Fig. 3. Refractive index profile and calculated optical mode distribution. Blue lines: DBSCH SQW LDs. Red lines: GRIN-DBSCH SQW LDs.

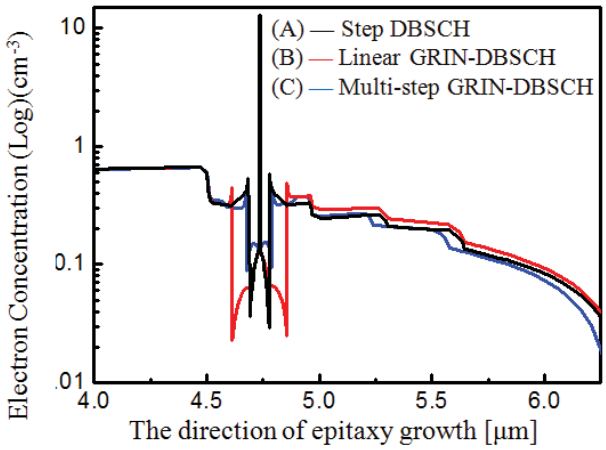

Fig. 4. Simulated carrier concentration for the 830-nm LDs with (a) step DBSCH, (b) linear GRIN-DBSCH, and (c) multistep GRIN-DBSCH waveguide layers.

chemical vapor (MOCVD) system. All the epitaxial layers were grown on (100) n-type GaAs substrates with Si as the n-type dopant, Zn as the p-type dopant in the cladding layers and C as the p-type dopant in the contact layer. The layer structures are shown in the Tabel I. Narrow stripe (5 μm) ridge waveguide laser structures were manufactured by chemical wet etching. Ti/Pt/Au and Au/Ge/Ni metallization were applied as p-side and n-side contacts, respectively. Laser chips were cleaved and covered with antioxidant passivation so that the cavity length was 500 μm. The facets were LR/HR coated by e-beam evaporation with Al_2O_3/TiO_2 multilayers and adopted deoxidizing treatment to enhance the COD level. The respective values of reflectivity were 25% and 97%. The devices were mounted on AlN heat sinks and packaged into copper TO-CANs.

III. Results and Discussion

The laser performance curves were measured with a CW driving current and FF patterns were taken by the CCD

TABLE I
LAYER SEQUENCES OF DBSCH LDS

	Layer Description	Version A (Step DBSCH)		Version B (Linear GRIN-DBSCH)		Version C (Multistep GRIN-DBSCH)	
		Al Composition x	Thickness [nm]	Al Composition x	Thickness [nm]	Al Composition x	Thickness [nm]
L12	GaAs P-cap layer	0	100	0	100	0	100
L11	AlGaAs P-cladding layer	0.54	1500	0.54	1500	0.54	1500
L10	AlGaAs grading layer	0.56–0.54	20	0.56–0.54	20	0.56–0.54	20
L9	AlGaAs barrier layer	0.56	90	0.56	90	0.56	90
L8	AlGaAs grading layer	–	–	0.39–0.56	116.9	0.45–0.56	80
L7	AlGaAs confinement layer	0.39	51.7	–	–	0.39–0.45	40
L6	InGaAsP SQW (λ = 830-nm)	–	50	–	50	–	50
L5	AlGaAs confinement layer	0.39	51.7	–	–	0.45–0.39	40
L4	AlGaAs grading layer	–	–	0.56–0.39	116.9	0.56–0.45	80
L3	AlGaAs barrier layer	0.56	90	0.56	120	0.56	120
L2	AlGaAs grading layer	0.53–0.56	20	0.53–0.56	20	0.53–0.56	20
L1	AlGaAs N-cladding layer	0.53	4500	0.53	4500	0.53	4500
L0	GaAs substrate	0	–	0	–	0	–

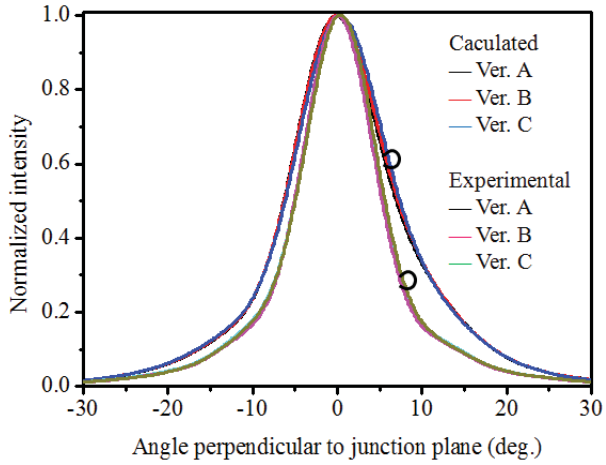

Fig. 5. Vertical far-field characteristics of SQW LDs fabricated from three DBSCH designs. Ver A: step. Ver B: linear. Ver C: multistep DBSCHs.

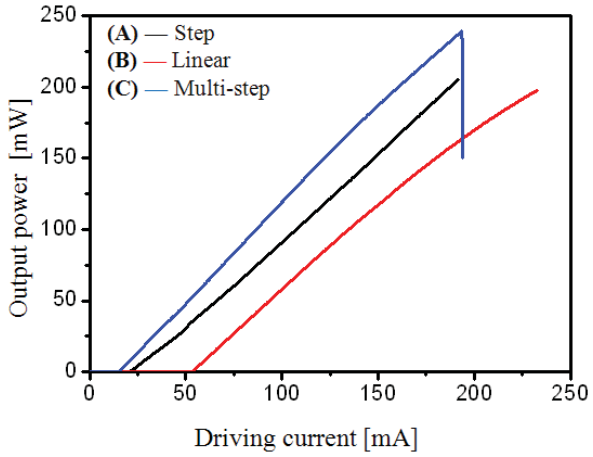

Fig. 6. L–I characteristics of narrow-stripe ridge waveguide LDs fabricated from three DBSCH designs.

camera at 100 mW output power at various temperature. The corresponding lateral FF beamwidths are in 9°–11° for all DBSCH laser types. When we modify the structure design of DBSCH LDs, the influence of the vertical FF divergences is more obvious than that of the lateral ones. As indicated in Fig. 5, only vertical fundamental transverse modes with no trace of higher order modes have been observed in the LDs, which are similar to the modeling results of the optical field distribution. The asymmetric Gaussian-like field profiles exhibiting in the far-filed patterns demonstrated the evidence of optical fields extending in to cladding layers, resulting in a narrow FWHM angle. As shown in Fig. 5, we can get narrower vertical divergence values of 13°–11° for all the DBSCH LDs compared with simulation results under a room temperature operation, which could be due to the influence of fabricated ridge structures.

For the power-current (L-I) measurement results shown in Fig. 6, experimental threshold current are 10.7, 21.5, and 52.5 mA for multi-step, step and linear GRIN DBSCH LDs, respectively. And the corresponding slope efficiencies are 1.12, 0.96, and 0.78. According to the calculated results of electron concentration distribution in Fig. 4, we can attribute a higher leakage current to a worse carrier confinement of LD. For the linear GRIN-DBSCH design, there are more carriers which would like to drift out of the confinement region and it leads to increase of leakage current more seriously. When we choose linear graded index profile as interlayers between QW and double-barrier layers, it showed a weaker carrier confinement within the active regions and the injected carriers might climb over the double-barrier easily. The phenomena of electron overflow will get worse as there is accumulation of more thermal energy around the QW during stimulated operation, especially under high-temperature or high-power CW operation. Therefore, we found that the threshold current of linear GRIN-DBSCH LD was much higher than those of the other two LDs. If we apply a pulsed current with 5% duty cycle to drive these LDs, the heat preservation in the active layers will be decreased effectively and it'll reduce the difference of pulsed threshold current between these three LDs. The corresponding values of measured threshold current

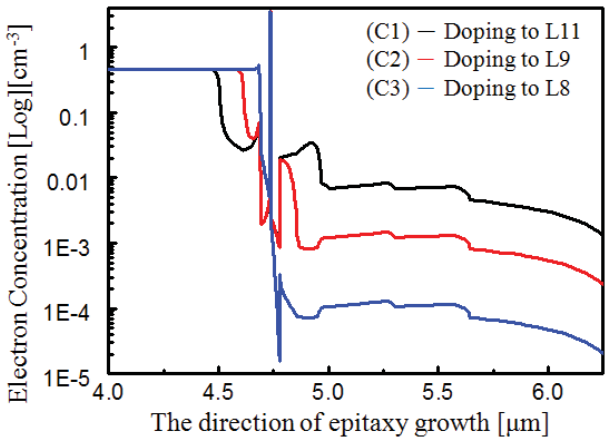

Fig. 7. Carrier concentration for the multistep GRIN-DBSCH LDs with p-type doping to (C1) claddnig layer, (c2) barrier layer, and (c3) inner grading layer.

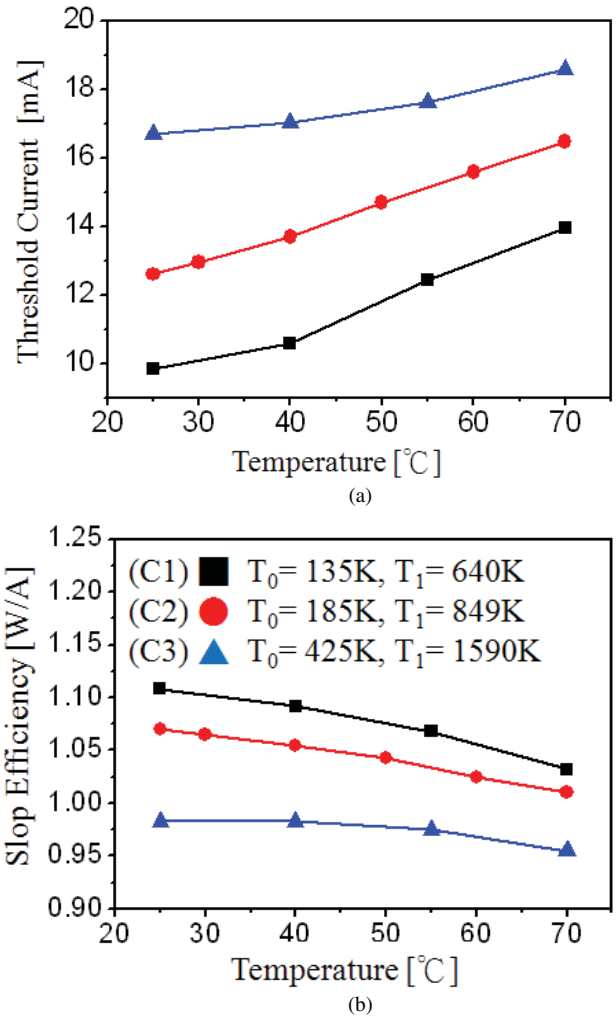

Fig. 8. Experimental (a) Ith and (b) SE as a function of temperature with p-type doping to (C1) claddnig layer, (c2) barrier layer, and (c3) inner grading layer.

are 10.5, 19.5, 35.5 mA for multi-step, step, and linear GRIN-DBSCH LDs, respectively. For the multi-step GRIN-DBSCH LD, we can get the smallest threshold current and the best slope efficiency when the vertical divergence angle was as narrow as 11.5°, which could be due to the good carrier confinement introduced by the multi-step grading interfaces.

Since the restrictions against leakage current is an important issue especially at high power and high temperature operation, we increased the p–type doping depth into the AlGaAs barrier layer to enhance the carrier confinement and improve the temperature characteristics based on the multi-step GRIN-DBSCH structure. Fig. 7 shows the simulated electron concentration for multi-step GRIN-DBSCH structures with various doping depth above the threshold. C1, C2 and C3 represent different p-type doping depth structures to the p-cladding layer (L11 shown in table I), barrier layer (L9 shown in table I) and inner grading layer (L8 shown in table I), respectively. For the LDs adopted a deeper doping profile closed to QW, we can find that the electron concentration in the p-type cladding layer was suppressed obviously. If we increase the depth of p-type doping, the quasi-Fermi level in the doped region will increase closer to the active layer; thus, the effective barrier height of double-barrier layers in the electronic band structure will rise Hence, it'll be helpful to restrain the electron overflow and lead to less carrier leakage. Comparing the electron concentration curves of three LDs, the "C3" LD doped into the inner grading layer shows a lowest leakage current in the p-type cladding layer due to the improvement of carrier confinement. The corresponding leakage current in the p-type cladding layer can be reduced form 327.7 A/cm^2 to 121.7 A/cm^2 when the p-type doping depth moved from L11 to L8. Hence, the deep doping design would be helpful for high power operation and for improving the device characteristic temperature.

Fig. 8 shows the measured threshold current (I_{th}) and slope efficiency (SE) as a function of operation temperature for these DBSCH LDs with several different p-type doping depth structures. Base on the above simulation results, we adjusted the p-type doping depth from cladding layers into the barrier layers to enhance the carrier confinement and raise the temperature characteristics. Although the deep p-type doping may have the benefit, decreasing the space between the p-type doping region and the QW active region may contribute to the increased probability of nonradiative recombination in the waveguide layers. The measured I_{th} therefore increased from 10.7 mA to 16.5 mA, and the slop efficiency was slightly deteriorated from 1.12 to 0.98 W/A.

The measures of temperature sensitivity can be defined by using the threshold current variation (T_0) and the slope efficiency variation (T_1). As raising temperature from 25° to 70°, the T_0 and T_1 of multi-step GRIN-DBSCH LD with a shallow doping stopped in the interface of cladding and confinement layers were estimated to be 135 K and 640 K. Better temperature characteristics can be obtained from sample with a deeper doping profile, which T_0 and T_1 were reaching as high as 425 K and 1590 K, respectively. In order to separate the thermal effect, we also provide the properties of temperature sensitivity measured during 5% duty cycle operation. The corresponding values of T_o/T_1 are 245 K/840 K, 295 K/1120 K, and 520 K/1980 K for C1, C2, and C3 LDs,

respectively. All the results are better than those operated with a CW driving current, especially the value of T_1. It proves the multi-step GRIN-DBSCH design with a doping profile into the barrier layer could effectively restrain the electron overflow and reduce leakage current under high temperature operation. The narrow-stripe ridge waveguide of GRIN-DBSCH LD with a narrow far-field pattern exhibited a maximum output power of 240 mW, corresponding to the COD level of power density of 21.5 MW/cm^2, which is calculated by the formula of $P_{COD} = (P_{max}/(W \cdot d/\Gamma)) \cdot (1+R)/(1-R)$ [12]. R is the front-facet reflectivity, P_{max} is the power at COD, d is the QW width, and Γ is the fraction of optical power residing in the QW. For a single-mode lateral waveguide, W is the full-width at half-maximum of the lateral spot. Given that the lateralbeam FWHM is about 10°, the calculated FWHM of the lateral spot size is close to 4.2 μm. It demonstrates capability for high-power applications in fiber lasers and solid state optical pumping sources.

IV. Conclusion

We have fabricated and demonstrated the characteristics of 830 nm band AlGaAs/InGaAsP LDs with different DBSCH deigns. The effects of the barrier thickness and height on the LD performance were calculated and discussed. As raising the barrier height or increasing the thickness, the optical mode would broaden, resulting in narrow vertical divergence beam in the far-field direction. In addition, the DBSCH design with a multi-step structure and modified doping profile has been proposed to further reduce vertical divergence emission and improve temperature characteristics. For GRIN-DBSCH LDs, vertical beam divergence can be reduced to 11.5° FWHM and CW I_{th} of 16.5 mA and SE of 0.98 W/A have been obtained at room temperature. The LDs can be driven at the maximum power density of 21.5 MW/cm^2 with high CW characteristic temperatures of T_0 and T_1 to be 425 K and 1590 K, respectively.

Acknowledgment

The authors would like to thank J.-T. Tsai, J.-de. Yu, J.-S Lee for device processing, Dr. H-C Lee and Dr. H-M Shieh at Union Optronics Corporation for technical support and on laser characteristics simulation.

References

[1] J. Sebastian, G. Beister, F. Bugge, F. Burhrandt, G. Erbert, H. G. Hänsel, R. Hülsewede, A. Knauer, W. Pitrroff, R. Staske, M. Shröder, H. Wenzel, M. Weyers, and G. Tränkle, "High power 810-nm GaAsP-AlGaAs diode lasers with narrow beam divergence," *IEEE J. Sel. Topics Quantum Electron.*, vol. 7, no. 2, pp. 334–339, Mar.–Apr. 2001.

[2] A. Knauer, G. Erbert, R. Staske, B. Sumpf, H. Wenzel, and M. Weyers, "High-power 808 nm lasers with a super-large optical cavity," *Semicond. Sci. Technol.*, vol. 20, no. 6, pp. 621–624, Jun. 2005.

[3] T. Hayakawa, M. Wada, F. Yamanaka, H. Asano, T. Kuniyasu, T. Ohgoh, and T. Fukunaga, "Effect of broad-waveguide structure in 0.8 um high-power InGaAsP/InGaP/AlGaAs lasers," *Appl. Phys. Lett.*, vol. 75, no. 13, pp. 1839–1841, Sep. 1999.

[4] J. K. Wade, L. J. Mawst, and D. Botez, "High continuous wave power 0.8 μm-band, Al-free active-region diode lasers," *Appl. Phys. Lett.*, vol. 70, no. 2, pp. 149–151, Mar. 1997.

[5] G. Yang, G. M. Smith, M. K. Davis, A. Kussmaul, D. A. S. Loeber, M. H. Hu, H.-K. Nguyen, C.-E. Zah, and R. Bhat, "High performance 980-nm ridge waveguide laser with a nearly circular beam," *IEEE Photon. Technol. Lett.*, vol. 16, no. 4, pp. 981–983, Apr. 2004.

[6] G. Lin, S.-T. Yen, C.-P. Lee, and D.-C. Liu, "Extremely small vertical far-field angle of InGaAs-AlGaAs quantum-well lasers with specially designed cladding structure," *IEEE Photon. Technol. Lett.*, vol. 8, no. 12, pp. 1588–1590, Dec. 1996.

[7] A. Malag and B. Mroziewicz, "Vertical beam divergence of double-barrier multi-quantum well (DBMQW) (AlGa)As heterostructure lasers," *J. Lightw. Technol.*, vol. 14, no. 6, pp. 514–1518, Jun. 1996.

[8] A. Malag, A. Kozlowska, and M. Wesolowski, "Effect of Al-content reduction in (AlGa)As cladding layers of MOVPE-grown high-power DBSQW laser diodes," in *Proc. 10th Eur. Workshop MOVPE Conf.*, Jun. 2003, pp. 235–238.

[9] Y. C. Chen, R. G. Waters, and R. J. Dalby, "Single-quantum-well laser with 11.2 degree transverse beam divergence," *Electron. Lett.*, vol. 26, no. 17, pp. 1348–1350, Aug. 1990.

[10] G. Lin, S. T. Yen, and C. P. Lee, "Extremely small vertical far-field angle of InGaAs-AlGaAs QW lasers with specially designed cladding structure," *IEEE Photon. Technol. Lett.*, vol. 8, no. 12, pp. 1588–1590, Dec. 1996.

[11] *LASTIP*, Crosslight Software, Inc., Burnaby, BC, Canada, 2005.

[12] J. K. Wade, L. J. Mawst, D. Botez, and J. A. Morris, "8.8 W CW power from broad-waveguide Al-free active-region ($\lambda = 805$ nm) diode lasers," *Electron. Lett.*, vol. 34, no. 11, pp. 1100–1101, May 1998.

Chih-Tsang Hung received the B.S. and M.S. degrees in material science and engineering from National Chiao Tung University, Hsinchu, Taiwan, in 2001 and 2003, respectively, and the Ph.D. degree with the Department of Photonics, National Chiao Tung University, in 2006.

He joined the Device Process and Development Division of the Union Optronics Corporation, Taiwan, in 2004, where he is currently the Manager of Research and Development Division from 2009 to 2012. He has investigated the development of III–V semiconductor lighting device, including design, epitaxial growth, chip process, and characterization of optoelectronic devices.

Tien-Chang Lu (M'07–SM'12) received the B.S. degree in electrical engineering from National Taiwan University, Taipei, Taiwan, in 1995, the M.S. degree in electrical engineering from the University of Southern California, Los Angeles, in 1998, and the Ph.D. in electrical engineering and computer science from National Chiao Tung University, Hsinchu, Taiwan, in 2004.

He was with the Union Optronics Corporation as a Manager of Epitaxy Department in 2004. Since August 2005, he has been with the Department of Photonics, National Chiao Tung University, as an Assistant Professor. In 2007, he was with the Department of Applied Physics, Ginzton Laboratory, Stanford University, Stanford, CA, as a Visiting Scholar. In 2009, he was an Associate Professor and the Director of the Institute of Lighting and Energy Photonics, National Chiao Tung University, from 2009 to 2011. He has been engaged in the low-pressure MOCVD epitaxial technique associated with various material systems as well as the corresponding process skills. He has been engaging in GaN-related research and has had several breakthroughs, such as first current injection blue VCSEL, photonic crystal surface emitting lasers, and microcavity exciton-polariton light emitters. He has authored or co-authored more than 150 international journal papers. His current research interests include design, epitaxial growth, process, characterization of optoelectronic devices, and structure design and simulations for optoelectronic devices using computer-aided software.

Dr. Lu is a recipient of the Exploration Research Award of Pan Wen Yuan Foundation in 2007, the Excellent Young Electronic Engineer Award in 2008, the Young Optical Engineering Award in 2010, and the MOC'11 Contribution Award in 2011.